Differential lncRNA/mRNA expression profiling and ceRNA network analyses in amniotic fluid from foetuses with ventricular septal defects

Huaming Wang [1], Xi Lin [2], Zecheng Wang [1], Shaozheng He [1], Bingtian Dong [1], Guorong Lyu [Corresp. 1, 3]

[1] Department of Ultrasound, Second Affiliated Hospital of Fujian Medical University, Quanzhou, Fujian, China

[2] Department of Diagnostic Radiology, Fujian Cancer Hospital of Fujian Medical University, Fuzhou, Fujian, China

[3] Collaborative Innovation Center of Maternal and Child Health Service Technology, Quanzhou Medical College, Quanzhou, Fujian, China

Corresponding Author: Guorong Lyu
Email address: lgr_feus@sina.com

Background. Long noncoding RNAs (lncRNAs) have been shown to be involved in the regulation of numerous biological processes in embryonic development. We aimed to explore lncRNA expression profiles in ventricular septal defects (VSDs) and reveal their potential roles in heart development.

Methods. Microarray analyses were performed to screen differentially expressed lncRNAs (DE-lncRNAs) and mRNAs (DE-mRNAs) in the amniotic fluid between the VSD group and the control group. Bioinformatics analyses were further used to identify the functional enrichment and signaling pathways of important mRNAs. Then, a coding–noncoding gene coexpression (CNC) network and competitive endogenous RNAs (ceRNA) network were drawn. Finally, qRT–PCR was performed to verify several hub lncRNAs and mRNAs in the network.

Results. A total of 710 DE-lncRNAs and 397 DE-mRNAs were identified in the VSD group. GO and KEGG analyses revealed that the DE-mRNAs were enriched in cardiac development-related biological processes and pathways, including cell proliferation, cell apoptosis, and the Sonic Hedgehog signaling pathway. Four VSD related mRNAs was used to construct the CNC network, which included 149 pairs of coexpressing lncRNAs and mRNAs. In addition, a ceRNA network, including 15 lncRNAs, 194 miRNAs, and 4 mRNAs, was constructed to reveal the potential regulatory relationship between lncRNAs and protein-coding genes. Finally, seven RNAs in the ceRNA network were validated, including IDS, NR2F2, GPC3, LINC00598, GATA3-AS1, PWRN1, and LINC01551.

Conclusion. Our study identified some lncRNAs and mRNAs may be potential biomarkers and therapeutic targets for foetuses with VSD, and described the lncRNA-associated ceRNA network in the progression of VSD.

1 **Differential lncRNA/mRNA expression profiling and ceRNA network analyses in amniotic**

2 **fluid from foetuses with ventricular septal defects**

3 Huaming Wang[1], Xi Lin[2], Zecheng Wang[1], Shaozheng He[1], Bingtian Dong[1], Guorong Lyu[1, 3]

5 [1] Department of Ultrasound, Second Affiliated Hospital of Fujian Medical University, Quanzhou,

6 Fujian, China;

7 [2] Department of Diagnostic Radiology, Fujian Cancer Hospital of Fujian Medical University,

8 Fuzhou, Fujian, China;

9 [3] Collaborative Innovation Center of Maternal and Child Health Service Technology, Quanzhou

10 Medical College.

12 Correspondence Author.

13 Guorong Lyu[1, 3]

14 Zhongshan load, Quanzhou, Fujian, 362000, China

15 E-mail address: lgr_feus@sina.com

17 **Abstract**

18 **Background.** Long noncoding RNAs (lncRNAs) have been shown to be involved in the regulation

19 of numerous biological processes in embryonic development. We aimed to explore lncRNA

20 expression profiles in ventricular septal defects (VSDs) and reveal their potential roles in heart

21 development.

22 **Methods.** Microarray analyses were performed to screen differentially expressed lncRNAs (DE-

23 lncRNAs) and mRNAs (DE-mRNAs) in the amniotic fluid between the VSD group and the control

24 group. Bioinformatics analyses were further used to identify the functional enrichment and

25 signaling pathways of important mRNAs. Then, a coding–noncoding gene coexpression (CNC)

26 network and competitive endogenous RNAs (ceRNA) network were drawn. Finally, qRT–PCR

27 was performed to verify several hub lncRNAs and mRNAs in the network.

28 **Results.** A total of 710 DE-lncRNAs and 397 DE-mRNAs were identified in the VSD group. GO

29 and KEGG analyses revealed that the DE-mRNAs were enriched in cardiac development-related

30 biological processes and pathways, including cell proliferation, cell apoptosis, and the Sonic

31 Hedgehog signaling pathway. Four VSD related mRNAs were used to construct the CNC network,

32 which included 149 pairs of coexpressing lncRNAs and mRNAs. In addition, a ceRNA network,

33 including 15 lncRNAs, 194 miRNAs, and 4 mRNAs, was constructed to reveal the potential

34 regulatory relationship between lncRNAs and protein-coding genes. Finally, seven RNAs in the

35 ceRNA network were validated, including IDS, NR2F2, GPC3, LINC00598, GATA3-AS1,

36 PWRN1, and LINC01551.

37 **Conclusion.** Our study identified some lncRNAs and mRNAs may be potential biomarkers and

38 therapeutic targets for foetuses with VSD and described the lncRNA-associated ceRNA network

39 in the progression of VSD.

40

41 **Introduction**

42 Ventricular septal defect (VSD) is one of the most prevalent foetal birth defects; it occurs in 4.3

43 of 1000 births and accounts for 39% of cases of congenital heart disease (CHD) in infants [1].

44 With the development of surgical procedures, some VSD infants have excellent long-term

45 survival; however, early intervention is key to reducing complications and improving prognosis

46 [2]. To formulate better diagnosis and treatment strategies for VSD, identification of the potential

47 inducements that cause abnormal foetal heart development is a prerequisite. According to

48 epidemiological investigations, genetic factors such as chromosomal or Mendelian syndromes

49 account for approximately 15% of all cases of CHD. The pathogenesis of the remaining 85% of

50 "sporadic" CHDs, which are not associated with chromosomal or Mendelian syndromes, has

51 proven intractable to genetic investigation [3]. These "sporadic" CHDs are presumed to be the

52 result of multiple genetic and environmental factors, suggesting incomplete penetrance. Epigenetic

53 factors reflect the interactions between genetic and environmental factors, which can be explained

54 by the differences in the genetic buffering capacity between individuals [4].

55   Recently, studies have shown that the development of the foetal heart is a complex and dynamic

56   process regulated by the correct spatiotemporal expression of noncoding RNAs (ncRNAs) [5].

57   Long noncoding RNAs (lncRNAs), which are the most abundant isoform of ncRNAs, have been

58   shown to participate in the regulation of tissue or cellular function by epigenetic mechanisms [6].

59   LncRNAs can activate or repress gene expression in several ways to affect foetal heart

60   development. For example, lncRNA uc.4 inhibits cell differentiation in heart development by

61   altering DNA methylation [7]. Enhancer lncRNAs are involved in the maintenance of cardiac stem

62   cell pluripotency and cardiomyocyte differentiation [8]. In addition, lncRNAs can act as

63   competitive endogenous RNAs (ceRNAs) to regulate the expression of downstream target genes

64   by competitively binding with miRNAs. Han et al. found that lncRNA-H19 facilitates Sox6

65   expression by binding with miR-19b to promote apoptosis and inhibit cell proliferation in P19CL6

66   cells during late-stage cardiac differentiation [9]. Several studies have shown that abnormal

67   expression of lncRNAs can cause corresponding cardiac defects. Wang et al. found that the

68   expression of lncRNA-HA117 in the myocardial tissue of children with Tetralogy of Fallot (ToF)

69   was increased and negatively correlated with prognosis [10]. Li et al. found that lncRNA-TUC40

70   expression was significantly increased in the heart tissues of VSD foetuses [11]. Based on these

71   findings, understanding the network structure and regulatory mechanism of lncRNAs could

72   profoundly impact the diagnosis and treatment of VSD.

73   Amniotic fluid (AF) is a complex and dynamic biological fluid, that is rich in foetal cell-free

74   DNA and RNA, and contains 100-200 times more foetal nucleic acids than maternal plasma [12].

75   Since AF is in direct contact with the foetal skin, urinary system, lungs, oropharynx, and

76   gastrointestinal tract, it can directly reflect the growth and development of the foetus [13].

77   Recently, studies have shown that AF provides dynamic ncRNA information about foetal

78   pathophysiological status inside the uterus. Vizitiu et al. showed that miR-99a was significantly

79   upregulated in the AF of foetuses with trisomy 21 syndrome [14]. Xie et al. found that AF-derived

80   miR-299-5p and miR-300 could be used as biomarkers to evaluate foetal kidney function and

81   prenatally diagnose congenital hydronephrosis [15]. In the clinic, AF is often collected to detect

82 chromosomal abnormalities and pregnancy-related complications. However, the relationship

83 between AF-derived lncRNAs and VSD remains to be fully exploited. Although our previous

84 publication showed that some lncRNAs were differentially expressed in the AF-derived exosomes

85 of VSD fetuses [16], there are still many VSD-related lncRNAs have not been excavated. In

86 addition, research has shown that some lncRNAs are enriched in exosomes, while others are barely

87 present, indicating that some lncRNAs are selectively sorted into exosomes [17]. Therefore, we

88 considered that lncRNA in AF supernatant can provide a more comprehensive analysis of foetal

89 development.

90   With the development of high-throughput analysis technology, it is possible to massively

91 analyze the transcriptome in parallel [18]. Compared with miRNAs whose functions are relatively

92 well studied, lncRNAs are still poorly annotated and contain repetitive elements, making the

93 analysis of RNA-seq data challenging [19]. Therefore, in this study, a lncRNA microarray was

94 used to screen differentially expressed lncRNAs (DE-lncRNAs) and mRNAs (DE-mRNAs) in AF

95 between the VSD group and the control group. Then, VSD-related lncRNAs and mRNAs were

96 selected by bioinformatics analyses and verified by qPCR. Based on these analyses, we predict the

97 potential role of lncRNAs in VSD and provide new biomarkers for the diagnosis and treatment of

98 VSD.

99

100 **Materials and methods**

101 **Patient recruitment and ethics statement**

102 In this study, pregnant women were recruited from the Second Affiliated Hospital of Fujian

103 Medical University. All pregnant women had indications for prenatal diagnosis and were assessed

104 by prenatal ultrasound and echocardiography. For safety and reasons of ethical constraints,

105 amniotic fluid sampling was only performed when pregnant women had indications for prenatal

106 diagnosis and without additional burden for the mother or fetus. Ultimately, 22 singleton pregnant

107 women aged 19-34 years between 20 and 22+6 weeks of gestation were included in the research.

108 Of these, 11 pregnant women who carried a VSD foetus were in the VSD group, and the other 11

109   pregnant women who carried a structurally normal foetus but had a high risk Down's screening

110   were in the control group. Both groups of pregnant women had no pregnancy complications and

111   poor life histories such as hypertension, diabetes, smoking, or alcoholism. All cases were tested

112   for chromosome anomalies by karyotype. Foetuses with abnormal karyotypes and extracardiac

113   major associated anomalies were excluded. There were no differences in maternal age, the number

114   of pregnancies, gestational age, or body mass index (BMI) between the VSD group and the control

115   group (P > 0.05). These clinical characteristics are shown in Table 1 and Table S1. This study was

116   performed in accordance with the principles of the World Medical Association Declaration of

117   Helsinki and licenced by the Ethics Committee of the Second Affiliated Hospital of Fujian Medical

118   University (NO. 2021-073).

119   **RNA extraction**

120   AF was extracted by amniocentesis from pregnant women and specimens with gross maternal

121   blood or meconium contamination were discarded. AF samples were centrifuged at 1600 × g for

122   10 min at 4 °C to remove amniocytes, and then supernatant samples were stored at -80 °C until

123   RNA extraction. Total RNA was extracted from AF supernatant using TRIzol LS Reagent

124   (Invitrogen, Carlsbad, CA) according to the manufacturer's protocol. Then, RNA quantity and

125   quality were measured by a NanoDrop ND-1000.

126   **RNA labelling and array hybridization**

127   In this study, we selected Arraystar Human LncRNA Microarray V5.0, which is designed for the

128   global profiling of human lncRNAs and protein-coding transcripts and can detect approximately

129   39,317 lncRNAs and 21,174 coding transcripts. The specific operations were as follows, each

130   RNA sample was amplified and transcribed into fluorescent cRNA along the entire length of the

131   transcripts without 3' bias utilizing a random priming method (Arraystar Flash RNA Labelling Kit,

132   Arraystar). The labelled cRNAs were purified using an RNeasy Mini Kit (Qiagen). The

133   concentration and specific activity of the labelled cRNAs (pmol Cy3/µg cRNA) were measured

134   by a NanoDrop ND-1000. 1 µg of each labelled cRNA was fragmented by adding 5 µl 10×Blocking

135   Agent and 1 µl of 25×Fragmentation Buffer, and then heating the mixture at 60 °C for 30 min.

136   Finally 25 μl 2×GE Hybridization buffer was added to dilute the labelled cRNA. 50 μl of

137   hybridization solution was dispensed into the gasket slide and assembled onto the lncRNA

138   expression microarray slide. The slides were incubated for 17 h at 65 °C in an Agilent

139   Hybridization Oven. The hybridized arrays were washed, fixed, and scanned using the Agilent

140   DNA Microarray Scanner (part number G2505C). The microarray work was performed by Kang

141   Chen Bio-tech, Shanghai, China.

142   **Data analysis**

143   Agilent Feature Extraction software (version 11.0.1.1) was used to analyse acquired array images.

144   Then, the GeneSpring GX v12.1 software package (Agilent Technologies) was used to perform

145   quantile normalization and subsequent data processing [20]. Differentially expressed lncRNAs

146   (DE-lncRNAs) and mRNAs (DE-mRNAs) between the two groups were identified through Fold

147   Change filtering and P value with the R-based limma software package [21]. Finally, heatmap and

148   volcano plots were generated for significantly differentially expressed genes using the "ggplot2

149   package" of R [22]. The threshold used to screen upregulated or downregulated lncRNAs and

150   mRNAs was a | fold-change | ≥ 2.0 (P < 0.05). The microarray data discussed in this paper have

151   been deposited in the NCBI Gene Expression Omnibus and are accessible with the GEO Series

152   accession   number   GSE204935

153   (https://www.ncbi.nlm.nih.gov/geo/query/acc.cgi?acc=GSE204935).

154   **Bioinformatics Analysis**

155   To identify the potential role of differentially expressed genes in VSD, Gene Ontology (GO)

156   annotation and Kyoto Encyclopedia of Genes and Genomes (KEGG) were used to illuminate the

157   functions of the DE-mRNAs [23-24]. GO analysis provides the key functional classifications for

158   DE-mRNAs, which include biological process (BP), cellular component (CC), and molecular

159   function (MF). KEGG reveals the relationship networks and disease information for DE-mRNAs.

160   Fisher's exact test was used to classify the GO and KEGG categories. The threshold of significance

161   was P value < 0.05 and FDR < 0.1.

162   **Construction of the CNC network and ceRNA network**

163   According to the above analysis, we selected core DE-mRNAs closely related to VSD for further

164   study. Based on the expression level of all DE-lncRNAs and core DE-mRNAs, the Pearson

165   correlation coefficient (PCC) was calculated by the "coXpress package" of R [25]. The DE-

166   lncRNAs and DE-mRNAs with PCC > 0.95 and P value < 0.05 were selected to construct the CNC

167   network.

168   To further explore the potential role of lncRNAs, a ceRNA (lncRNA–miRNA–mRNA) network

169   based on core DE-mRNAs was constructed. First, the miRcode database (v11) was used to predict

170   miRNA targets on lncRNAs [26], and the TargetScan database (v7.2) was used to predict miRNA

171   targets on mRNAs [27]. The thresholds for the algorithms were conservation scores >50 for

172   miRcode, and target scores ≥70 for TargetScan. Then, the lncRNA–miRNA–mRNA interaction

173   network was constructed using the overlapping miRNAs that harboured both lncRNA and mRNA

174   binding targets. The Cytoscape (v2.8.2) program was used to construct and visualize the CNC

175   network and ceRNA network [28].

176   **Quantitative real-time reverse transcription PCR (qRT–PCR)**

177   Total RNA was extracted from AF supernatant using TRIzol LS Reagent (Invitrogen, Carlsbad,

178   CA) and then cDNA was synthesized from 1 ug of total RNA using PrimeScript™ RT reagent Kit

179   with gDNA Eraser (Takara, Dalian, China). cDNA was amplified and quantified using TB Green®

180   Premix Ex Taq™ II (Takara, Dalian, China). The cycling parameters were as follows: the first

181   step, 95 °C for 30 s; the second step, 95 °C for 5 s and 60 °C for 34 s, for 40 cycles; and the third

182   step, for melting 95 °C for 15 s, 60 °C for 60 s and 95 °C for 15 s. Each sample was measured in

183   triplicate and the sequences of the primers used are shown in Table S2. The obtained data of

184   lncRNAs and mRNAs expression levels were calculated and normalized by the $2^{-\Delta\Delta Ct}$ method as

185   follows: $\Delta Ct_{(test/control)}$ = average value $Ct_{(target\ gene)}$ - average value $Ct_{(GAPDH)}$; $\Delta\Delta Ct = \Delta Ct_{(test/control)}$

186   - average value $\Delta Ct_{(control)}$.

187   **Statistical analysis**

188   Heatmaps and volcano plots based on the expression levels of genes were generated and visualized

189   using R statistical software. Fisher's exact test was employed to evaluate the significance of GO

190   or KEGG enrichment. The expression levels of lncRNAs and mRNAs were calculated via an

191   unpaired t-test between the VSD and control groups. All quantitative data are expressed as the

192   mean ± SD and were analysed using SPSS 21.0 (SPSS Inc. USA). $P < 0.05$ was considered to

193   indicate a statistically significant difference [29].

194

195   **Results**

196   **Differentially expressed lncRNAs and mRNAs**

197   To evaluate the differential expression of AF-derived lncRNAs and mRNAs between the VSD and

198   control groups, AF supernatant from 5 VSD foetuses and 5 control foetuses was obtained by a

199   random method and subjected to microarray analysis. Box plots were used to compare the

200   intensities and quality of microarray data (Figure 1A, 1B). The result showed that the distributions

201   of intensities in different samples were similar after normalization. A volcano plot was used to

202   assess the variation in lncRNA and mRNA expression between the two groups (Figure 1C, 1D).

203   Finally, hierarchical clustering was used to show distinguishable lncRNA and mRNA expression

204   profiles (Figure 1E, 1F). With the cut-off criteria of a | fold change | ≥ 2 and P value <0.05, 710

205   lncRNAs were significantly differentially expressed between the two groups, of which 240 were

206   upregulated and 470 were downregulated in the VSD group. Similarly, 397 mRNAs were

207   significantly differentially expressed between the two groups, of which 106 were upregulated and

208   291 were downregulated in the VSD group. the expression level of the up- and down-regulated

209   DE-mRNAs and DE-lncRNAs was showed in Table S3 and S4.

210   **Characteristics of differentially expressed lncRNAs and mRNAs**

211   To further analyze the DE-lncRNAs and DE-mRNAs, we summarized some general

212   characteristics of these genes, such as type distribution, genomic location distribution, and length.

213   As shown in Figure 2 A and 2B, in both up- and down-regulated lncRNAs, intergenic lncRNAs

214   are the largest types, and intron sense overlapping lncRNAs are the least type. The results of

215   positioning showed that up- and down-regulated lncRNAs were mainly distributed on

216   chromosomes 1 and 2, respectively. While, both the up- and down-regulated mRNAs were mainly

217 distributed on chromosomes 1(Figure 2C, 2D and Figure S1). The length distribution showed that

218 most DE-lncRNAs were distributed within 0.5-1 kb; however, the DE-mRNAs were mainly

219 distributed at 2-4 kb in length. These results prompt that chromosome 1 and 2 may contain more

220 genes related to the VSD process, and compared with other types of lncRNA, intergenic lncRNAs

221 are more critical in the formation of cardiac defects.

222 **GO and pathway analysis**

223 To explore the mechanisms and pathways during the progression of VSD, the biological meaning

224 and systematic features of the significant DE-mRNAs were first annotated by GO ontology. A

225 total of 713 GO terms were significantly enriched. The top ten terms of the GO ontology results

226 are shown in Figure 3A. BP analysis indicated that the DE-mRNAs were enriched in heart

227 development, cell adhesion, and regulation of cell proliferation. CC analysis indicated that the DE-

228 mRNAs were enriched in cell junction, cell-substrate junction, and extracellular matrix. MF

229 analysis indicated that the DE-mRNAs were enriched in kinase regulator activity and protein-

230 containing complex binding.

231 KEGG pathway analysis was used to investigate the wire diagrams of molecular interactions,

232 reactions, and relations related to the DE-mRNAs. The top ten enriched KEGG pathways are

233 shown in Figure 3B including the Sonic Hedgehog signaling pathway (Shh), the

234 Phosphatidylinositol signaling system, apoptosis, and the regulation of the actin cytoskeleton. In

235 addition, KEGG disease enrichment analysis showed that DE-mRNAs were involved in congenital

236 malformations, cardiovascular diseases, and nervous system diseases (Figure 3C). Of these, the

237 most enriched disease was congenital malformations with 24 genes annotated with this term. These

238 results show that DE-mRNAs are rich in biological activities and signal pathways related to heart

239 development, including cell adhesion, cell proliferation and apoptosis, tissue development, and

240 regulation of Shh signaling pathway.

241 **Construction of the CNC network and ceRNA network**

242 According to GO and KEGG analysis, four core mRNAs, including IDS, ID1, NR2F2, and GPC3,

243 were selected to construct a CNC network because they are closely connected to cardiac biology.

244   Among the coexpression analysis, 4 core mRNAs and 141 lncRNAs comprise the CNC network,

245   which includes 149 pairs of coexpressing lncRNAs and mRNAs. As shown in Figure 4A, a core

246   mRNA could have a correlation with many lncRNAs, and most of these relationship pairs

247   presented a positive correlation. To our knowledge, ceRNAs play important roles in the cis-

248   regulation of lncRNAs. Therefore, we constructed a ceRNA network to reveal the regulatory

249   mechanism between lncRNAs and mRNAs in the CNC network. In the ceRNA network, the

250   miRcode and TargetScan databases were used to predict miRNA targets on lncRNAs and mRNAs,

251   respectively. A total of 194 overlapping miRNAs were selected to construct the ceRNA network.

252   To better show the specific ceRNA network, we constructed the network of up-regulated and

253   down-regulated genes, respectively. Eventually, the down-regulated ceRNA network includes 11

254   lncRNAs, 129 miRNAs, and 2 mRNAs, while, the up-regulated ceRNA network includes 4

255   lncRNAs, 79 miRNAs, and 2 mRNAs. (Figure 4B and 4C).

256   **Validation of RNA expression by qPCR**

257   According to the GO/KEGG analysis and CNC/ceRNA network, we examined the expression of

258   four core mRNAs (IDS, ID1, NR2F2, and GPC3) and five lncRNAs (AL022323.5, LINC00598,

259   GATA3-AS1, PWRN1, and LINC01551) to confirm the reliability of our microarray results. To

260   increase the accuracy of the results, qPCR was performed in 5 VSD and 5 healthy samples used

261   for microarray, and in 6 additional VSD and 6 additional healthy samples. The qPCR results

262   showed that seven RNAs (IDS, NR2F2, GPC3, LINC00598, GATA3-AS1, PWRN1, and

263   LINC01551) were consistent with the results of microarray analysis, while two RNAs (ID1, and

264   AL022323.5) were not significantly different between the two groups (Table 2 and Figure 5).

265

266   **Discussion**

267   The development of the heart is a complex and dynamic process regulated by a variety of ncRNAs

268   and mRNAs. Although transcriptomic analyses of CHD have been reported in several studies,

269   information about lncRNA expression and the mechanism by which lncRNAs contribute to the

270   development of VSD is limited. In the present study, we compared the expression profiles of the

271 lncRNAs and mRNAs between the VSD group and the control group using the microarray

272 technique. We identified 710 dysregulated lncRNAs and 397 dysregulated mRNAs and

273 summarized their general characteristics. Through bioinformatics analysis, we found that these

274 dysregulated genes were enriched in cardiac development-related biological processes and

275 pathways. Subsequently, a CNC network and ceRNA network were constructed to predict the

276 mechanisms and functional roles of gene regulation. The qPCR results confirmed that NR2F2,

277 GATA3-AS1, and PWRN1 were upregulated, and IDS, GPC3, LINC00598, and LINC01551 were

278 downregulated in VSD.

279   To understand the role of lncRNAs in the pathogenesis of VSD, we have generated an integrated

280 analysis of dysregulated lncRNAs and mRNAs. GO and KEGG analyses showed that DE-mRNAs

281 were enriched in cell adhesion, cell proliferation and apoptosis, tissue development, and regulation

282 of Shh signaling pathway. The overall growth of the heart during embryogenesis involves multiple

283 overlapping stages of cell proliferation, apoptosis, and morphogenesis [30]. The decreased

284 proliferation or increased apoptosis of cardiomyocyte will lead to cardiac defects, including

285 developmental defects in heart valves and double outlet right ventricle [31-32]. In addition, cell

286 adhesion is essential for maintaining the integrity of the chambers and compartments of the heart

287 [33]. Shh is a key signaling pathway during cardiac cell regeneration and heart ontogenesis.

288 Abolishing the Shh signaling pathway for a brief period during embryogenesis is sufficient to bring

289 about irreversible cardiac deformities [34]. The above studies have showed that the biological

290 activities of DE-mRNAs are closely related to cardiac biology and may be the molecular

291 mechanism of VSD development.

292   Through biological information analysis and literature review, four mRNA, including IDS, ID1,

293 NR2F2, and GPC3, were selected for the next study. These mRNAs are related to cardiac

294 development. For instance, IDS contributes to aberrant heart development and cardiomyocyte

295 differentiation disorder by affecting the catabolism of GAGs [35]. ID1 encodes a transcription

296 regulator that is involved the differentiation of cardiac precursors by regulating apoptosis and

297 proliferation of cardiomyocyte [36]. Pathogenic mutations in the NR2F2 and GPC3 will lead to

298   many cardiac defects, such as VSD, Tetralogy of Fallot and double outlet right ventricle [37, 38].

299   Interestingly, these four genes are related to the Shh signaling pathway. ID1 can activate the Shh

300   signaling pathway to maintain cell stemness [39]. Silencing IDS and NR2F2 can significantly

301   inhibit the expression of Shh downstream target genes [34, 40]. The loss of GPC3 function

302   selectively reduces Shh signaling in cardiomyocyte [41]. Therefore, we consider that these DE-

303   mRNAs may affect the biological activity of cardiomyocyte through the Shh signaling pathway,

304   leading to the formation of CHD.

305   How lncRNAs regulate molecular and cellular functions remains largely elusive. One possibility

306   is that lncRNAs regulate the expression levels of coding RNAs and add intricacy to the regulatory

307   network of cardiac gene expression [42, 43]. Therefore, we selected lncRNAs related to the above

308   mRNAs for further analysis. First, according to the ceRNA hypothesis, we constructed a CNC

309   network and ceRNA network to reveal the potential regulatory relationship between lncRNAs and

310   protein-coding genes. Second, we selected conserved lncRNAs in the network for qPCR

311   validation. Finally, we identified 4 lncRNAs that were differentially expressed between the VSD

312   group and the normal group, including LINC00598, GATA3-AS1, PWRN1, and LINC01551.

313   Although the mechanism of these four lncRNAs in CHD is not clear, many research have shown

314   that they are related to the cell cycle, cell proliferation and apoptosis. For instance, knockdown of

315   LINC00598 can inhibit cell proliferation by inducing G0/G1 cell cycle stagnation [44].

316   Knockdown of GATA3-AS1 and LINC01551 markedly limited cell invasion abilities, cell

317   proliferation, and cell viability [45, 46]. PWRN1 overexpression suppress xenograft growth in

318   vivo and cancer cell migration in vitro [47]. Recently, numerous studies have revealed that

319   lncRNA can indirectly regulate mRNA expression levels by competitively binding to a miRNA

320   response element [48]. Moreover, Published reports have confirmed that lncRNA can lead to CHD

321   through this regulation mechanism. For example, FGD5-AS1 is an hub lncRNA in the TOF heart

322   ceRNA network and can regulate SMAD4 by binding with hsa-miR-421 [49]. It is worth

323   mentioning that the 4 verified lncRNAs as a miRNA sponge are widely reported in cancers, such

324   as the GATA3-AS1/miR-495-3p/CENPU axis in breast cancer [50], and the PWRN1/miR-214-5p

325   axis in osteosarcoma [51]. Based on the above analysis, we speculated that lncRNAs with ceRNA

326   activity may be regulate the cell cycle, cell proliferation, and apoptosis by regulating heart-related

327   mRNA and lead to the development of the CHD.

328   The genes mentioned above seem to be critical for the occurrence of CHD, and gene regulation

329   mediated by ncRNAs may provide new strategies for the treatment of CHD. In the past few years,

330   several ncRNA-based drugs have been in phase II or III clinical development. Most of these drugs

331   regulate the expression of downstream genes by mimicking or antagonizing the function of ncRNA

332   to achieve therapeutic effects [52]. For example, an intravenous injection of a miR-378 mimic

333   prevents excessive myocardial fibrosis in a mouse model of transverse aortic constriction [53].

334   Although some potential therapeutic targets were found in our study, the clinical application of

335   ncRNA still faces key challenges, including tolerability, delivery, specificity, and potential side

336   effects [54]. Therefore, a detailed understanding of the biological and molecular mechanisms

337   underlying ncRNA-mediated CHD development is key to translating such knowledge into clinical

338   usage.

339   There are several limitations of this study that should be discussed. First, a small sample size is

340   the main limitation of this study. In addition, the assessment of the correlation between lncRNAs

341   and mRNAs was based on a comprehensive analysis of 5 pairs of samples, which may have

342   inevitable biases. Therefore, we need to increase the sample size for future research. Second, the

343   exact influence mechanism of mRNAs and lncRNAs validated by qRT–PCR on VSD has not been

344   investigated in depth. The molecular functions and molecular mechanisms mediated by lncRNAs

345   still need to be verified in vitro and in vivo. Third, due to the diverse biological functions of

346   lncRNAs, the lncRNAs that we have not investigated further should not be considered to be

347   unrelated to CHD.

348

349   **Conclusion**

350   In summary, our study provides a comprehensive profile of AF-derived lncRNAs and mRNAs

351   in VSD foetuses and further reveals that these DE-mRNAs and DE-lncRNAs contribute to the

352   development of VSD via cell adhesion, cell proliferation, cell apoptosis, and the Shh signaling

353   pathway. Finally, we constructed a ceRNA network to elucidate the molecular mechanism of

354   lncRNAs in VSD development.

355   **Competing Interests**

356   The authors declare there are no competing interests.

357   **Author Contributions**

358   Huming Wang conceived and designed the experiments, performed the experiments, analyzed the

359   data, prepared figures and/or tables, authored or reviewed drafts of the paper, and approved the

360   final draft.

361   Xi Lin and Zecheng Wang conceived and designed the experiments, prepared figures and/or tables,

362   and approved the final draft.

363   Shaozheng HE and Bingtian Dong performed the experiments, authored or reviewed drafts of the

364   article, and approved the final draft.

365   Guorong Lyu planned and managed this project, organized the collaboration, analyzed the data,

366   edited this manuscript, and approved the final draft.

367   **Human Ethics**

368   The following information was supplied relating to ethical approvals (i.e., approving body and any

369   reference numbers):

370   The study was conducted in accordance with the Declaration of Helsinki (as revised in 2013). The

371   study was approved by the Medical Ethics Committee of the Second Affiliated Hospital of Fujian

372   Medical University (NO. 2021-073).

373   **Data Availability**

374   The following information was supplied regarding data availability:

375   The raw RNA microarray data is available on the Gene Expression Omnibus (GEO) site

376   (https://www.ncbi.nlm.nih.gov/geo/) (GEO: GSE204935).

377   **Funding**

378   This work was supported by the Qihang Fund of Fujian Medical University [grant number

379   2020QH2039], Quanzhou City Science & Technology Program of China [grant number
380   2021C059R], and the Natural Science Foundation of Fujian Province [grant number 2020J01129].
381

382   **Reference**

383   1. Liu Y, Chen S, Zühlke L, Black GC, Choy MK, Li N, Keavney BD. 2019. Global birth
384   prevalence of congenital heart defects 1970-2017: updated systematic review and meta-
385   analysis of 260 studies. Int J Epidemiol 48:455-463.

386   2. Jeon B, Kim DH, Kwon BS, Choi ES, Park CS, Yun TJ. 2020. Surgical treatment of tetralogy
387   of Fallot in symptomatic neonates and young infants. J Thorac Cardiovasc Surg 159:1466-
388   1476.e2.

389   3. Hopkins MK, Dugoff L, Kuller JA. 2019. Congenital Heart Disease: Prenatal Diagnosis and
390   Genetic Associations. Obstet Gynecol Surv 74:497-503.

391   4. Lim TB, Foo SYR, Chen CK. 2021. The Role of Epigenetics in Congenital Heart Disease.
392   Genes (Basel) 12:390.

393   5. Chahal G, Tyagi S, Ramialison M. 2019. Navigating the non-coding genome in heart
394   development and Congenital Heart Disease. Differentiation 107:11-23.

395   6. Ye S, Chen W, Ou C, Chen MS. 2022. RNA sequencing reveals novel LncRNA/mRNAs co-
396   expression network associated with puerarin-mediated inhibition of cardiac hypertrophy in
397   mice. PeerJ 10:e13144.

398   7. Zhang Q, Feng M, Zhang H, Xu J, Zhang L, Wang X, Cheng Z, Qian L. 2018. Long noncoding
399   RNA uc.4 inhibits cell differentiation in heart development by altering DNA methylation. J
400   Cell Biochem 10.1002/jcb.28084.

401   8. Devaux Y, Zangrando J, Schroen B, Creemers EE, Pedrazzini T, Chang CP, Dorn GW 2nd,
402   Thum T, Heymans S; Cardiolinc network. 2015. Long noncoding RNAs in cardiac
403   development and ageing. Nat Rev Cardiol 12:415-425.

404   9. Han Y, Xu H, Cheng J, Zhang Y, Gao C, Fan T, Peng B, Li B, Liu L, Cheng Z. 2016.
405   Downregulation of long non-coding RNA H19 promotes P19CL6 cells proliferation and

406   inhibits apoptosis during late-stage cardiac differentiation via miR-19b-modulated Sox6. Cell

407   Biosci 6:58.

408   10. Wang Q, Wang Z, Wu C, Pan Z, Xiang L, Liu H, Jin X, Tong K, Fan S, Jin X. 2018. Potential

409   association of long noncoding RNA HA117 with tetralogy of Fallot. Genes Dis 5:185-190.

410   11. Li H, Jiang L, Yu Z, Han S, Liu X, Li M, Zhu C, Qiao L, Huang L. 2017. The Role of a Novel

411   Long Noncoding RNA TUC40- in Cardiomyocyte Induction and Maturation in P19 Cells. Am

412   J Med Sci 354:608-616.

413   12. Kamath-Rayne BD, Smith HC, Muglia LJ, Morrow AL. 2014. Amniotic fluid: the use of high-

414   dimensional biology to understand fetal well-being. Reprod Sci 21:6-19.

415   13. O'Neill K, Alexander J, Azuma R, Xiao R, Snyder NW, Mesaros CA, Blair IA, Pinney SE.

416   2018. Gestational Diabetes Alters the Metabolomic Profile in 2nd Trimester Amniotic Fluid in

417   a Sex-Specific Manner. Int J Mol Sci 19:2696.

418   14. Vizitiu AC, Stambouli D, Pavel AG, Muresan MC, Anastasiu DM, Bejinar C, Alexa A, Marian

419   C, Sirbu IO, Sima L. 2019. Mature miR-99a Upregulation in the Amniotic Fluid Samples from

420   Female Fetus Down Syndrome Pregnancies: A Pilot Study. Medicina (Kaunas) 55:728.

421   15. Xie J, Zhou Y, Gao W, Li Z, Xu Z, Zhou L. 2017. The relationship between amniotic fluid

422   miRNAs and congenital obstructive nephropathy. Am J Transl Res 9:1754-1763.

423   16. Yang H, Yang S, Shen H, Wu S, Ruan J, Lyu G. 2021. Construction of the amniotic fluid-

424   derived exosomal ceRNA network associated with ventricular septal defect. Genomics

425   113:4293-4302.

426   17. Sun Z, Yang S, Zhou Q, Wang G, Song J, Li Z, Zhang Z, Xu J, Xia K, Chang Y, Liu J, Yuan

427   W. 2018. Emerging role of exosome-derived long non-coding RNAs in tumor

428   microenvironment. Mol Cancer 17:82.

429   18. Liguori M, Nuzziello N, Licciulli F, Consiglio A, Simone M, Viterbo RG, Creanza TM,

430   Ancona N, Tortorella C, Margari L, Grillo G, Giordano P, Liuni S, Trojano M. 2018.

431   Combined microRNA and mRNA expression analysis in pediatric multiple sclerosis: an

432   integrated approach to uncover novel pathogenic mechanisms of the disease. Hum Mol Genet

433   27:66-79.

434   19. Weirick T, Militello G, Müller R, John D, Dimmeler S, Uchida S. 2016. The identification and

435   characterization of novel transcripts from RNA-seq data. Brief Bioinform 17:678-685.

436   20. Zahurak M, Parmigiani G, Yu W, Scharpf RB, Berman D, Schaeffer E, Shabbeer S, Cope L.

437   2007. Pre-processing Agilent microarray data. BMC Bioinformatics 8:142.

438   21. Diboun I, Wernisch L, Orengo CA, Koltzenburg M. 2006. Microarray analysis after RNA

439   amplification can detect pronounced differences in gene expression using limma. BMC

440   Genomics 7:252.

441   22. H. Wickham. 2016. ggplot2: Elegant Graphics for Data Analysis. Springer-Verlag New York,.

442   23. The Gene Ontology Consortium. 2017. Expansion of the Gene Ontology knowledgebase and

443   resources. Nucleic Acids Res ;45(D1).

444   24. Kanehisa M, Goto S. 2000. KEGG: kyoto encyclopedia of genes and genomes. Nucleic Acids

445   Res 28:27-30.

446   25. Watson M. 2006. CoXpress: differential co-expression in gene expression data. BMC

447   Bioinformatics 7:509.

448   26. Jeggari A, Marks DS, Larsson E. 2012. miRcode: a map of putative microRNA target sites in

449   the long non-coding transcriptome. Bioinformatics 28:2062-2063.

450   27. Agarwal V, Bell GW, Nam JW, Bartel DP. 2015. Predicting effective microRNA target sites

451   in mammalian mRNAs. Elife 4:e05005.

452   28. Shannon P, Markiel A, Ozier O, Baliga NS, Wang JT, Ramage D, Amin N, Schwikowski B,

453   Ideker T. 2003. Cytoscape: a software environment for integrated models of biomolecular

454   interaction networks. Genome Res 13:2498-2504.

455   29. Mushquash C, O'Connor BP. 2006. SPSS and SAS programs for generalizability theory

456   analyses. Behav Res Methods 38:542-7.

457   30. Yu R, Li Z, Zhang C, Song H, Deng M, Sun L, Xu L, Che X, Hu X, Qu X, Liu Y, Zhang Y.

458   2019. Elevated limb-bud and heart development (LBH) expression indicates poor prognosis

459   and promotes gastric cancer cell proliferation and invasion via upregulating Integrin/FAK/Akt

460   pathway. PeerJ 7:e6885.

461   31. Miao Y, Tian L, Martin M, Paige SL, Galdos FX, Li J, Klein A, Zhang H, Ma N, Wei Y,

462   Stewart M, Lee S, Moonen JR, Zhang B, Grossfeld P, Mital S, Chitayat D, Wu JC, Rabinovitch

463   M, Nelson TJ, Nie S, Wu SM, Gu M. 2020. Intrinsic Endocardial Defects Contribute to

464   Hypoplastic Left Heart Syndrome. Cell Stem Cell 27:574-589.e8.

465   32. Zhang S, Song Z, An L, Liu X, Hu XW, Naz A, Zhou R, Guo X, He L, Zhu H. 2019. WD40

466   repeat and FYVE domain containing 3 is essential for cardiac development. Cardiovasc Res

467   115:1320-1331.

468   33. Li J, Liu Y, Jin Y, Wang R, Wang J, Lu S, VanBuren V, Dostal DE, Zhang SL, Peng X. 2017.

469   Essential role of Cdc42 in cardiomyocyte proliferation and cell-cell adhesion during heart

470   development. Dev Biol 421:271-283.

471   34. Costa R, Urbani A, Salvalaio M, Bellesso S, Cieri D, Zancan I, Filocamo M, Bonaldo P, Szabò

472   I, Tomanin R, Moro E. 2017. Perturbations in cell signaling elicit early cardiac defects in

473   mucopolysaccharidosis type II. Hum Mol Genet 26:1643-1655.

474   35. Matsuhisa K, Imaizumi K. 2021. Loss of Function of Mutant IDS Due to Endoplasmic

475   Reticulum-Associated   Degradation: New   Therapeutic   Opportunities   for

476   Mucopolysaccharidosis Type II. Int J Mol Sci 22:12227.

477   36. Hu W, Xin Y, Hu J, Sun Y, Zhao Y. 2019. Inhibitor of DNA binding in heart development and

478   cardiovascular diseases. Cell Commun Signal 17:51.

479   37. Duong TB, Ravisankar P, Song YC, Gafranek JT, Rydeen AB, Dohn TE, Barske LA, Crump

480   JG, Waxman JS. 2018. Nr2f1a balances atrial chamber and atrioventricular canal size via BMP

481   signaling-independent and -dependent mechanisms. Dev Biol 434:7-14.

482   38. Capurro MI, Xu P, Shi W, Li F, Jia A, Filmus J. 2008. Glypican-3 inhibits Hedgehog signaling

483   during development by competing with patched for Hedgehog binding. Dev Cell 14:700-711.

484   39. Sun Y, Lai X, Yu Y, Li J, Cao L, Lin W, Huang C, Liao J, Chen W, Li C, Yang C, Ying M,

485   Chen Q, Ye Y. 2019. Inhibitor of DNA binding 1 (Id1) mediates stemness of colorectal cancer

486   cells through the Id1-c-Myc-PLAC8 axis via the Wnt/β-catenin and Shh signaling pathways.

487   Cancer Manag Res 11:6855-6869.

488 40. Li Y, Xia Y, Wang Y, Mao L, Gao Y, He Q, Huang M, Chen S, Hu B. 2013. Sonic hedgehog

489   (Shh) regulates the expression of angiogenic growth factors in oxygen-glucose-deprived

490   astrocytes by mediating the nuclear receptor NR2F2. Mol Neurobiol 47:967-975.

491 41. Liu YC, Wierbowski BM, Salic A. 2022. Hedgehog pathway modulation by glypican 3-

492   conjugated heparan sulfate. J Cell Sci 135:jcs259297.

493 42. Ye S, Chen W, Ou C, Chen MS. 2022. RNA sequencing reveals novel LncRNA/mRNAs co-

494   expression network associated with puerarin-mediated inhibition of cardiac hypertrophy in

495   mice. PeerJ 10:e13144.

496 43. Kim NJ, Lee KH, Son Y, Nam AR, Moon EH, Pyun JH, Park J, Kang JS, Lee YJ, Cho JY.

497   2021. Spatiotemporal expression of long noncoding RNA Moshe modulates heart cell lineage

498   commitment. RNA Biol 18:640-654.

499 44. Jeong OS, Chae YC, Jung H, Park SC, Cho SJ, Kook H, Seo S. 2016. Long noncoding RNA

500   linc00598 regulates CCND2 transcription and modulates the G1 checkpoint. Sci Rep 6:32172.

501 45. Liu Y, Xu G, Li L. 2021. LncRNA GATA3-AS1-miR-30b-5p-Tex10 axis modulates

502   tumorigenesis in pancreatic cancer. Oncol Rep 45:59.

503 46. Xue MY, Cao HX. 2020. LINC01551 promotes metastasis of nasopharyngeal carcinoma

504   through targeting microRNA-132-5p. Eur Rev Med Pharmacol Sci 24:3724-3733.

505 47. Jiang J, Wang X, Lu J. 2020. PWRN1 Suppressed Cancer Cell Proliferation and Migration in

506   Glioblastoma by Inversely Regulating hsa-miR-21-5p. Cancer Manag Res 12:5313-5322.

507 48. Salmena L, Poliseno L, Tay Y, Kats L, Pandolfi PP. 2011. A ceRNA hypothesis: the Rosetta

508   Stone of a hidden RNA language?. Cell 146:353-358.

509 49. Zhang X, Gao Y, Zhang X, Zhang X, Xiang Y, Fu Q, Wang B, Xu Z. 2021. FGD5-AS1 Is a

510   Hub lncRNA ceRNA in Hearts With Tetralogy of Fallot Which Regulates Congenital Heart

511   Disease Genes Transcriptionally and Epigenetically. Front Cell Dev Biol 9:630634.

512 50. Lin S, Zhao M, Lv Y, Mao G, Ding S, Peng F. 2021. The lncRNA GATA3-AS1/miR-495-

513   3p/CENPU axis predicts poor prognosis of breast cancer via the PLK1 signaling pathway.

514   Aging (Albany NY) 13:13663-13679.

515 51. Shi J, Fu Q, Yang P, Yi Z, Liu S, Wang K. 2020. Long noncoding RNA PWRN1 is lowly

516   expressed in osteosarcoma and modulates cancer proliferation and migration by targeting hsa-

517   miR-214-5p. IUBMB Life 72:2444-2453.

518 52. Pei Y, Zhou B, Liu X. 2022. The long non-coding RNA rhabdomyosarcoma 2-associated

519   transcript exerts anti-tumor effects on lung adenocarcinoma via ubiquitination of SOX9. Ann

520   Transl Med 10:10.

521 53. Yuan J, Liu H, Gao W, Zhang L, Ye Y, Yuan L, Ding Z, Wu J, Kang L, Zhang X, Wang X,

522   Zhang G, Gong H, Sun A, Yang X, Chen R, Cui Z, Ge J, Zou Y. 2018. MicroRNA-378

523   suppresses myocardial fibrosis through a paracrine mechanism at the early stage of cardiac

524   hypertrophy following mechanical stress. Theranostics 8:2565-2582.

525 54. Winkle M, El-Daly SM, Fabbri M, Calin GA. 2021. Noncoding RNA therapeutics - challenges

526   and potential solutions. Nat Rev Drug Discov 20:629-651.

Table 1: Clinical characteristics of VSD group and control group.

1   Table 1: Clinical characteristics of VSD group and control group.

Characteristics	VSD group (n = 11)	Control group (n = 11)	P value
Maternal age (years)	30.82±3.9	31.64±5.2	0.681
Gestational age (weeks)	21.18±0.9	20.64±0.8	0.144
Number of deliveries	1.91±0.8	2.09±0.8	0.614
Body mass index (kg/m^2)	22.09±1.0	21.82±1.3	0.273

Table2: qPCR Detection of differential expression of lncRNAs and mRNAs in VSD group and control group.

1   Table 2: Differential expression of lncRNAs and mRNAs in VSD group and control group by
2   qPCR.

RNA	VSD group (n = 11)		Control group (n = 11)		Fold Chang	P value
	Mean	SD	Mean	SD		
IDS	0.42	0.22	1.05	0.34	0.40	0.000
ID1	1.93	1.25	1.26	0.93	1.53	0.164
NR2F2	3.89	1.63	1.45	1.62	2.68	0.002
GPC3	0.47	0.29	1.14	0.66	0.41	0.006
AL022323.5	1.20	1.51	2.99	4.16	0.40	0.193
LINC00598	0.44	0.34	1.36	1.09	0.32	0.015
GATA3-AS1	3.88	2.06	1.43	1.04	2.71	0.002
PWRN1	5.60	2.97	1.11	0.56	5.05	0.000
LINC01551	0.34	0.14	1.02	0.18	0.33	0.000

Figure 1

Figure 1: Different expression profiles of lncRNAs and mRNAs between VSD and control samples.

(A, B) Box plots of lncRNAs and mRNAs showing the distributions of intensities from all samples. The distributions were similar after normalization. (C, D) Volcano map of lncRNAs and mRNAs. The horizontal green line represents P=0.05, and the vertical green lines correspond to 2.0-fold up and down. Data points in black indicates genes with no significant difference, red indicates upregulated genes, and green indicates downregulated genes. (E, F) Heatmap of lncRNAs and mRNAs. The abscissa represents different samples, and the ordinate represents different genes. The red boxes indicate upregulated genes, and the green boxes indicate downregulated genes. Genes expressed at the average level are in black. "T" stands for VSD sample, "N" stands for control sample.
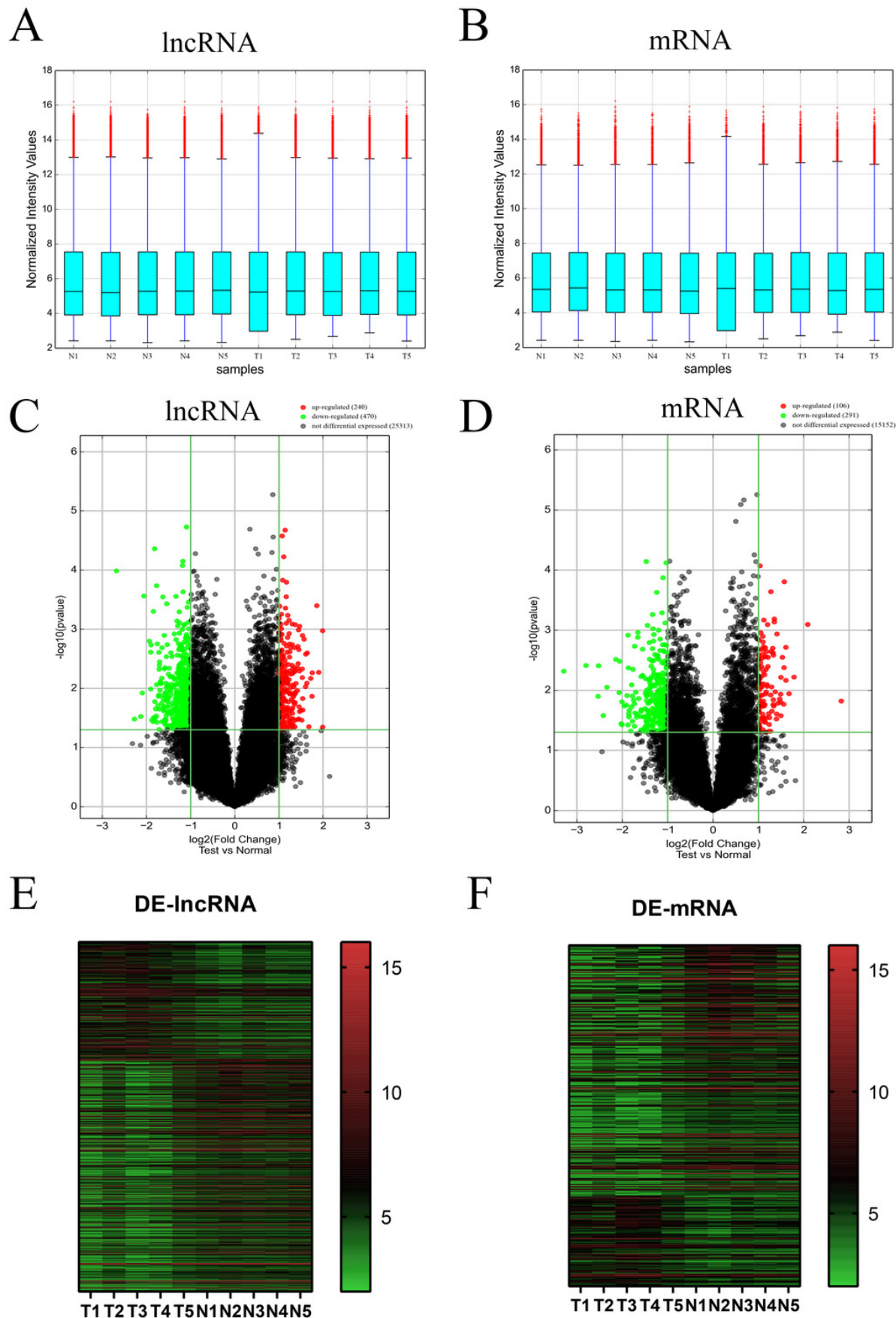
Figure 2

Figure 2: Characteristics of the differentially expressed lncRNAs and mRNAs.

(A, B) Type distribution of the down- and up-regulated lncRNAs. (B, C) Distribution of lncRNA and mRNA genomic locations. Red indicates upregulated genes, and green indicates downregulated genes.
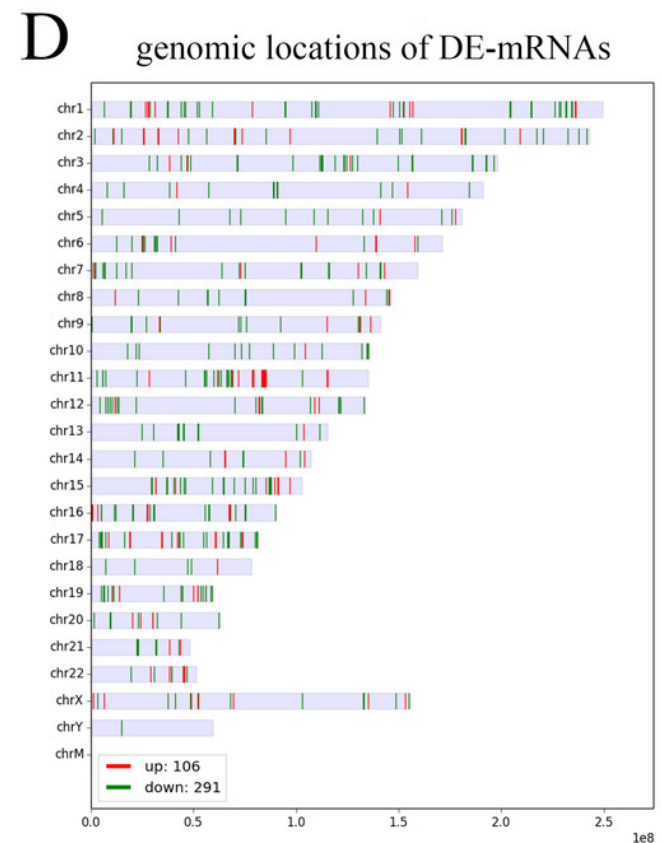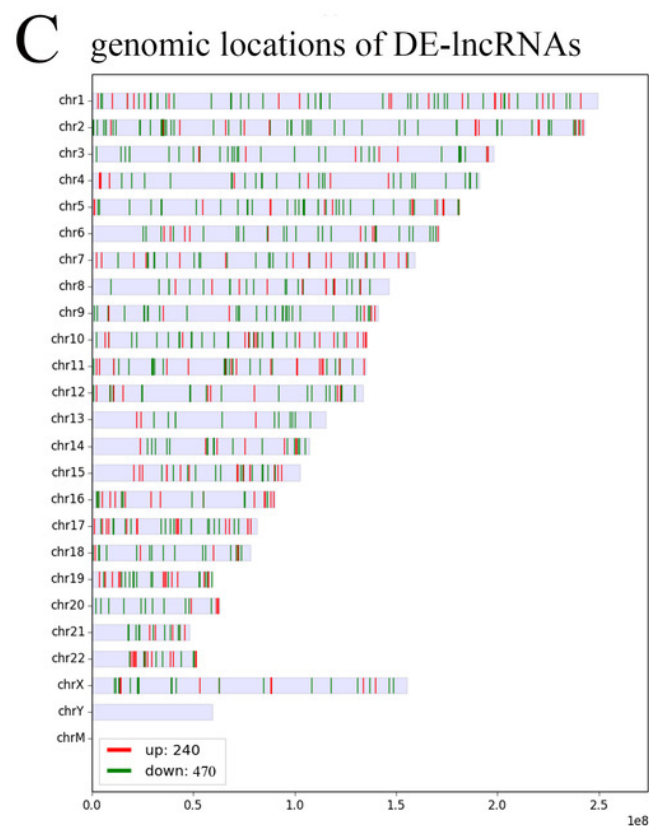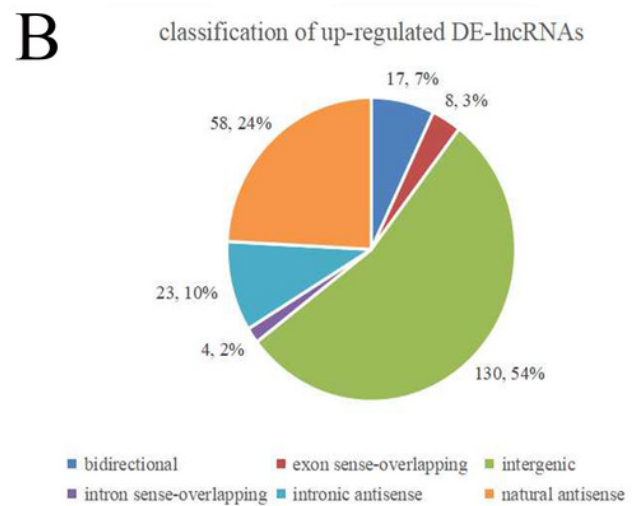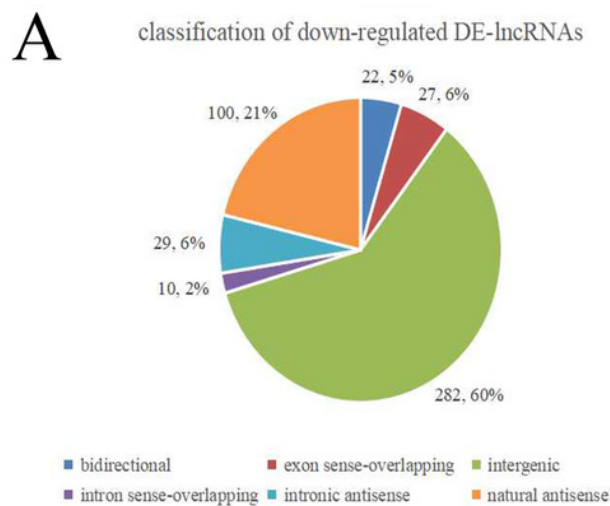
Figure 3

Figure 3: Bioinformatics analysis of DE-mRNAs.

(A) Top ten GO enriched terms for the DE-mRNAs between the VSD and control groups. The abscissa represents the GO term name, and the ordinate represents the enrichment score. (B) Top ten enriched KEGG pathways of DE-mRNAs between the VSD and control groups. The abscissa represents the enrichment score, and the ordinate represents the KEGG pathway name. (C) KEGG disease enrichment analysis of DE-mRNAs. The abscissa represents the gene ratio, and the ordinate represents the KEGG disease name. The size and colour of the bubbles represent the number of genes enriched in the disease and the value of−log10 (P value), respectively. GO: Gene Ontology; BP: Biological Process; CC: Cellular Component; MF: Molecular Function; KEGG: Kyoto Encyclopedia of Genes and Genomes.
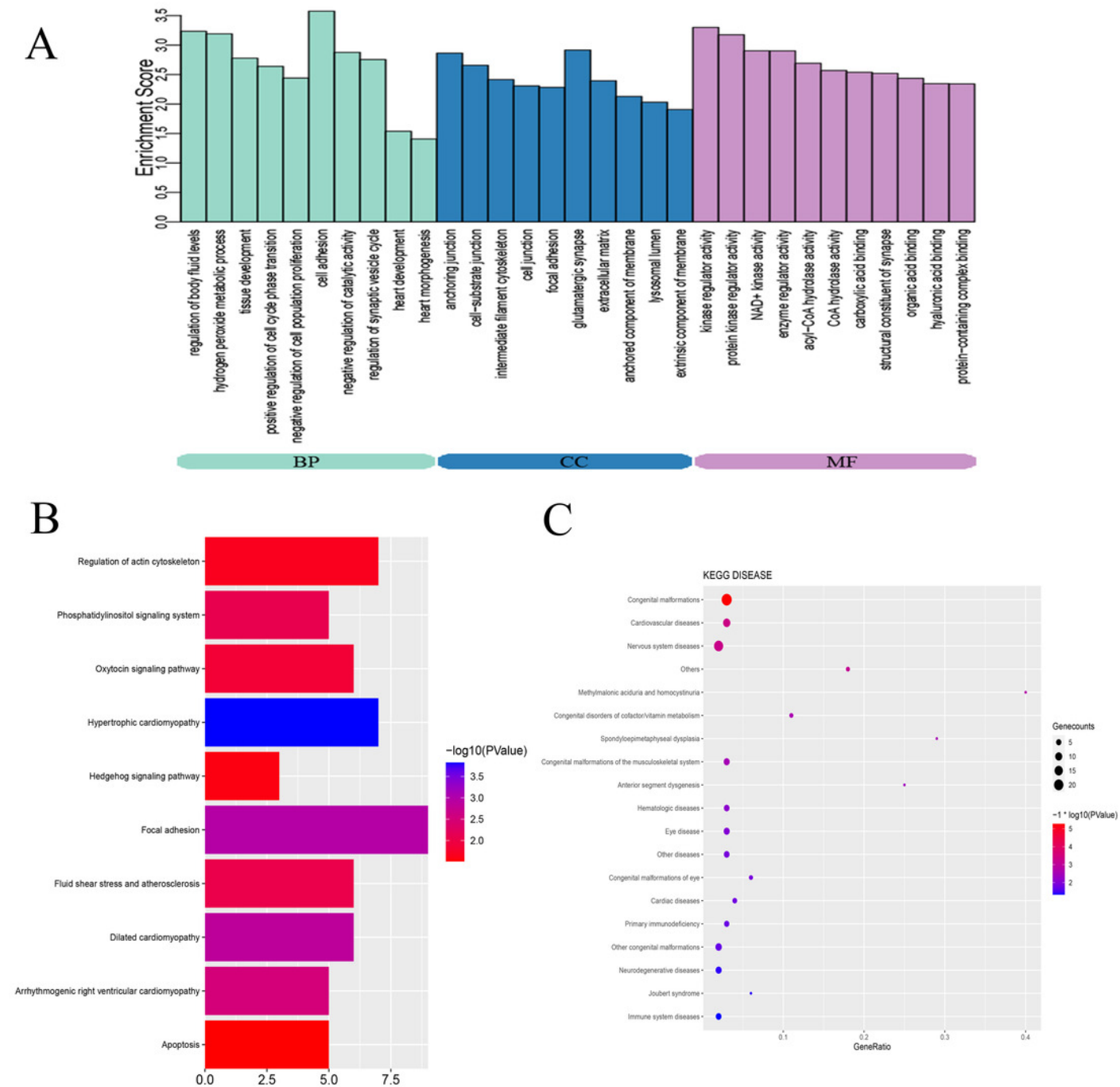
Figure 4

Figure 4: CNC network and ceRNA network.

(A) CNC network. The ellipse represents mRNAs and the diamond represents lncRNAs. Red and green represent up- and downregulated RNAs, respectively. The solid line indicates a positive correlation, and the dashed line indicates a negative correlation. (B, C) ceRNA network of downregulated and upregulated genes. The ellipse represents mRNAs, the diamond represents lncRNAs, and the V shape represents miRNAs. Red and green represent up- and downregulated RNAs, respectively.
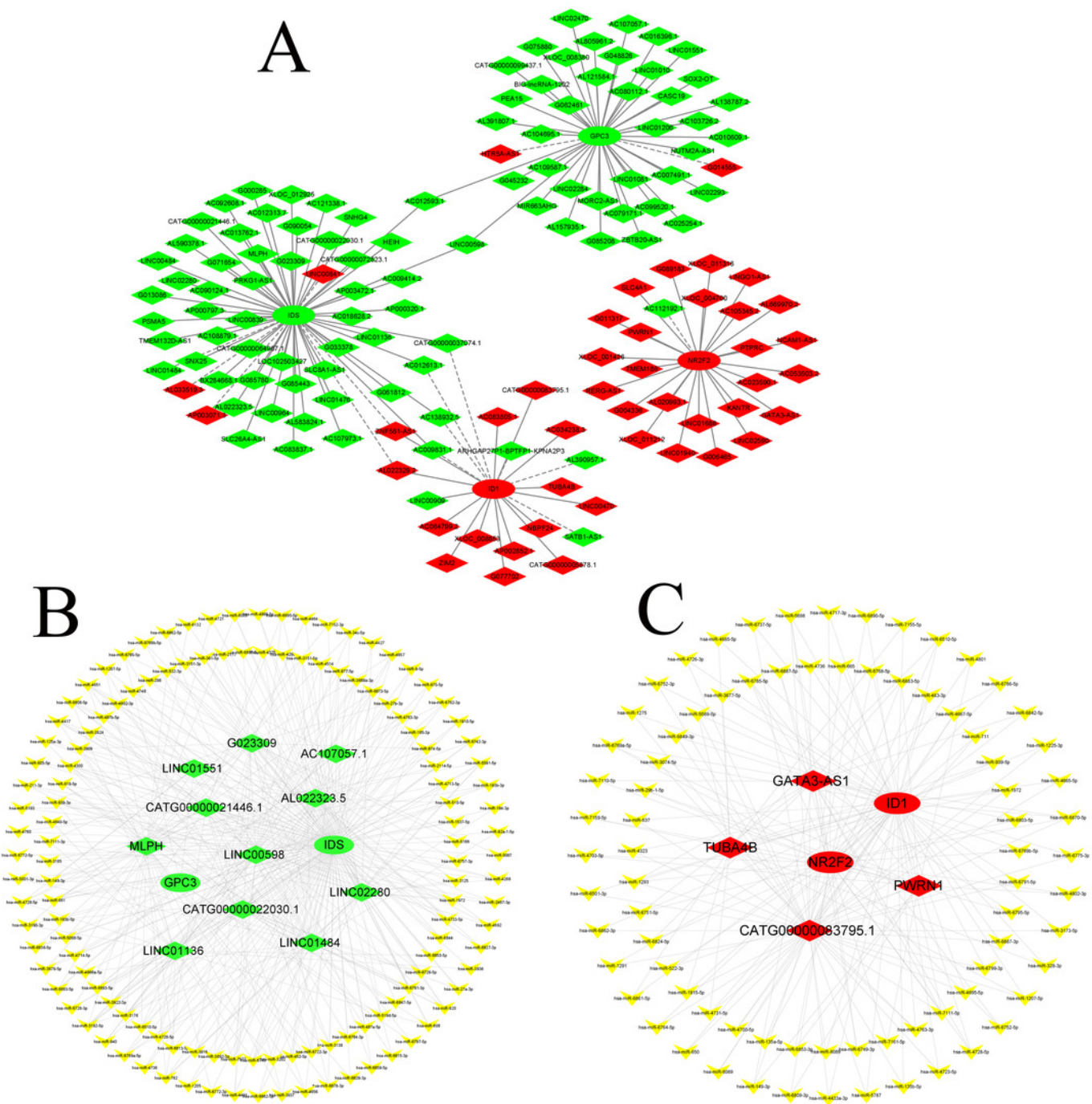
Figure 5

Figure 5: Relative expression levels of candidate lncRNAs and mRNAs from the RNA array and qPCR.

(A) Fold change of 7 candidate RNAs from the RNA array. Red represents upregulated genes, while green represents downregulated genes. (B-H) Expression levels of 7 candidate RNAs from qPCR. * indicates p<0.05 and ** indicates p<0.01.